THE JOURNAL OF BIOLOGICAL CHEMISTRY
Vol. 279, No. 50, Issue of December 10, pp. 51749–51759, 2004

Printed in U.S.A.

The Methylerythritol Phosphate Pathway Is Functionally Active in All Intraerythrocytic Stages of *Plasmodium falciparum**[S]

Received for publication, July 23, 2004, and in revised form, September 22, 2004
Published, JBC Papers in Press, September 27, 2004, DOI 10.1074/jbc.M408360200

María B. Cassera‡§, Fabio C. Gozzo¶, Fabio L. D'Alexandri‡§, Emilio F. Merino‡§, Hernando A. del Portillo‡‖, Valnice J. Peres‡, Igor C. Almeida‡‖, Marcos N. Eberlin¶, Gerhard Wunderlich‡, Jochen Wiesner, Hassan Jomaa**, Emilia A. Kimura‡, and Alejandro M. Katzin‡‖‡‡**

*From the ‡Department of Parasitology, Institute of Biomedical Sciences, University of São Paulo, 05508-900 São Paulo, Brazil, the ¶Thomson Mass Spectrometry Laboratory, Institute of Chemistry, State University of Campinas, 13083-970 Campinas, Brazil, and the **Institute of Biochemistry, Justus-Liebig-University, D-35392, Giessen, Germany*

Two genes encoding the enzymes 1-deoxy-D-xylulose-5-phosphate synthase and 1-deoxy-D-xylulose-5-phosphate reductoisomerase have been recently identified, suggesting that isoprenoid biosynthesis in *Plasmodium falciparum* depends on the methylerythritol phosphate (MEP) pathway, and that fosmidomycin could inhibit the activity of 1-deoxy-D-xylulose-5-phosphate reductoisomerase. The metabolite 1-deoxy-D-xylulose-5-phosphate is not only an intermediate of the MEP pathway for the biosynthesis of isopentenyl diphosphate but is also involved in the biosynthesis of thiamin (vitamin B_1) and pyridoxal (vitamin B_6) in plants and many microorganisms. Herein we report the first isolation and characterization of most downstream intermediates of the MEP pathway in the three intraerythrocytic stages of *P. falciparum*. These include, 1-deoxy-D-xylulose-5-phosphate, 2-*C*-methyl-D-erythritol-4-phosphate, 4-(cytidine-5-diphospho)-2-*C*-methyl-D-erythritol, 4-(cytidine-5-diphospho)-2-*C*-methyl-D-erythritol-2-phosphate, and 2-*C*-methyl-D-erythritol-2,4-cyclodiphosphate. These intermediates were purified by HPLC and structurally characterized via biochemical and electrospray mass spectrometric analyses. We have also investigated the effect of fosmidomycin on the biosynthesis of each intermediate of this pathway and isoprenoid biosynthesis (dolichols and ubiquinones). For the first time, therefore, it is demonstrated that the MEP pathway is functionally active in all intraerythrocytic forms of *P. falciparum*, and *de novo* biosynthesis of pyridoxal in a protozoan is reported. Its absence in the human host makes both pathways very attractive as potential new targets for antimalarial drug development.

Malaria is one of the leading causes of morbidity and mortality in the tropics, with 300 to 500 million clinical cases and 1.5 to 2.7 million deaths per year. Nearly all fatal cases are caused by *Plasmodium falciparum*. The resistance of this parasite to conventional antimalarial drugs such as chloroquine is growing at an alarming rate and therefore new efficient drugs are urgently needed (1–3).

In all organisms studied so far, the biosynthesis of isoprenoids such as dolichol, cholesterol, and ubiquinones depends on the condensation of the different numbers of isopentenyl diphosphate (IPP)[1] and dimethylallyl diphosphate units. In mammals and fungi, these units are derived from the classical mevalonate pathway (4). However, in higher plants, in several algae, in some eubacteria, and in *P. falciparum* the 2-*C*-methyl-D-erythritol-4-phosphate (MEP) pathway was described as the alternative non-mevalonate pathway for the synthesis of IPP (for reviews, see Refs. 5–10). This pathway starts with the condensation of pyruvate and glyceraldehyde 3-phosphate, which yields 1-deoxy-D-xylulose-5-phosphate (DOXP) as a key metabolite (11–17). The DOXP reductoisomerase then catalyzes the simultaneous intramolecular rearrangement and reduction of DOXP to form MEP (18–22). The activity of this enzyme is specifically inhibited by fosmidomycin (23). Several reaction steps are necessary for the conversion of MEP to IPP. The downstream intermediates of MEP for this pathway are: 4-(cytidine-5-diphospho)-2-*C*-methyl-D-erythritol (CDP-ME) (24), 4-(cytidine-5-diphospho)-2-*C*-methyl-D-erythritol-2-phosphate (CDP-MEP), 2-*C*-methyl-D-erythritol-2,4-cyclodiphosphate (ME-2,4-cPP) (25, 26), and 4-hydroxy-3-methylbut-2-enyl pyrophosphate (27–31). IPP and dimethylallyl diphosphate are synthesized through independent routes in the late steps of the non-mevalonate pathway (32). These units are used for the biosynthesis of ubiquinones and dolichols, and for the prenylation of proteins and other products (33–35).

Based on the sequence data provided by the malaria genome project (plasmodb.org), Jomaa and co-workers (21) identified two genes in *P. falciparum* that encode key enzymes of the MEP pathway: 1-deoxy-D-xylulose-5-phosphate synthase and 1-deoxy-D-xylulose-5-phosphate reductoisomerase. They also demonstrated that an amino-terminal signal sequence in 1-de-

* This work was supported in part by grants from the Fundação de Amparo à Pesquisa do Estado de São Paulo, Conselho Nacional de Desenvolvimento Científico e Tecnológico, PRONEX, and UNDP/World Bank/WHO-TDR, European Commission INCO-Dev, 5th Framework Programme Contract ICA4-CT-2001-10078. The costs of publication of this article were defrayed in part by the payment of page charges. This article must therefore be hereby marked "*advertisement*" in accordance with 18 U.S.C. Section 1734 solely to indicate this fact.

[S] The on-line version of this article (available at http://www.jbc.org) contains Figs. Data I and II.

§ Supported by Fundação de Amparo à Pesquisa do Estado de São Paulo.

‖ Research fellows from Conselho Nacional de Desenvolvimento Científico e Tecnológico.

‡‡ To whom correspondence should be addressed: Laboratory of Malaria, Dept. of Parasitology, Institute of Biomedical Sciences, University of São Paulo, Av. Lineu Prestes 1374, 05508-900, São Paulo, SP, Brazil. Tel.: 55-11-3091-7330; Fax: 55-11-3091-7417; E-mail: amkatzin@icb.usp.br.

[1] The abbreviations and trivial names used are: IPP, isopentenyl diphosphate; MEP, 2-*C*-methyl-D-erythritol-4-phosphate; DOXP, 1-deoxy-D-xylulose-5-phosphate; DOX, 1-deoxy-D-xylulose; CDP-ME, 4-(cytidine-5-diphospho)-2-*C*-methyl-D-erythritol; CDP-MEP, 4-(cytidine-5-diphospho)-2-*C*-methyl-D-erythritol-2-phosphate; ME-2,4-cPP, 2-*C*-methyl-D-erythritol-2,4-cyclodiphosphate; HPLC, high-performance liquid chromatography; ESI-QTOF-MS, ESI-quadrupole time-of-flight mass spectrometry; Q_n, Coenzyme Q_n.

oxy-D-xylulose-5-phosphate reductoisomerase targeted the enzyme to apicoplasts. Furthermore, this group demonstrated that fosmidomycin and FR900098 are able to inhibit growth of *P. falciparum* in culture and to cure mice infected with the related malaria parasite, *Plasmodium vinckei* (21). Recent field trials in humans have also demonstrated the effectiveness of fosmidomycin in the treatment of human malarial infections (36, 37). Afterward, Rohdich and colleagues (38) described the isolation of 2-*C*-methyl-D-erythritol-2,4-cyclodiphosphate synthase from *P. falciparum*.

In several organisms, DOXP is also used for both thiamin (vitamin B_1) (39) and pyridoxal (vitamin B_6) biosynthesis (40–42). The term vitamin B_6 is used to refer collectively to the compound pyridoxine (pyridoxol) and its vitamers pyridoxal, pyridoxamine, and their phosphorylated derivatives. Vitamin B_6 is essential for all organisms and plays a key role as a co-factor in many metabolic conversions of amino acids. All organisms have an efficient salvage pathway that interconvert between the various vitameric forms and their phosphorylated derivatives. Plants, fungi, bacteria, archaebacteria, and protists synthesize pyridoxine, for which two independent and exclusive biosynthetic machineries exist. One machinery consists of the *pdxA*, *pdxB*, *pdxJ*, and *pdxH* genes, restricted to some eubacteria like *Escherichia coli*. The other machinery is characterized by the presence of two genes, *pdx1* and *pdx2*, and seems to be broadly distributed in plants, fungi, archaebacteria, and some eubacteria (43, 44). The *pdx1* and *pdx2* gene sequences are completely unrelated to the *E. coli* genes. The pathway for *de novo* vitamin B_6 biosynthesis was extensively characterized in *E. coli* (40, 45–48). Very recently, the enzymatic function of the *pdx2* gene product has been demonstrated, with glutamine amidotransferase activity (49, 50). The enzymatic activity of the product encoded by *pdx1* was recently inferred by Wetzel and colleagues (51) using cross-complementation analysis to determine a functional relationship between *pdx1* and *pdxJ*. It has been suggested that *pdx1* is involved in the pyridoxine ring closure reaction. The *P. falciparum* genome contains a *pdx1* homologue (PlasmoDB ID code MAL6P1.215) suggesting that the parasite could possibly synthesize pyridoxine.

Because of their absence in human cells, both the MEP pathway and perhaps the *de novo* synthesis of vitamin B_6 are excellent molecular targets for the development of new antimalarial drugs. Furthermore, in-depth knowledge of the biosynthesis of intermediates could refine the search for news drugs aimed at the inhibition of each intermediate of the corresponding pathways. On the other hand, the presence of genes or their transcripts does not necessarily prove that the corresponding proteins are metabolically active. For this reason, the active metabolic pathway must be demonstrated. In this report, we demonstrate by biochemical and mass spectrometric analyses the presence of most of the intermediates of the MEP pathway and an active *de novo* biosynthesis of pyridoxine in blood stage forms of the malaria parasite.

EXPERIMENTAL PROCEDURES

Materials

RPMI 1640 medium, RPMI 1640 medium without glucose and methionine, Hepes, hypoxanthine, glucose, gentamicin, LiOH, BaOH, saponin, D-sorbitol, geraniol, farnesol, geraniolgeraniol, dolichol 11, prenol C_{40-60}, prenol C_{80-110}, Coenzyme Q_7, Coenzyme Q_{10}, Tris, EDTA, SDS, 2-mercaptoethanol, Triton X-100, phenylmethylsulfonyl fluoride, iodoacetamide, sodium *p*-tosyllysine chloromethyl ketone, and leupeptin were purchased from Sigma. Coenzyme Q_9 and pyridoxine (vitamin B_6) were purchased from Fluka (Buchs, Switzerland). Coenzyme Q_8 was isolated from *E. coli* by extraction with hexane and further purification by high-performance liquid chromatography (HPLC) as described by Okamoto and co-workers (52). AlbuMax I2 was obtained from Invitrogen. A sample of chemically synthesized 1-deoxy-D-xylulose, used as a standard substance for HPLC peak identification, was a kind gift from D. Arigoni (Laboratorium Für Organische Chemie, Eidgenössische Technische Hochschule, Zürich, Switzerland). The standards MEP, CDP-ME, CDP-MEP, ME-2,4-cPP, [2-^{14}C]DOXP (50 mCi/mmol), and the antibiotic fosmidomycin were kindly provided by H. Jomaa (Biochemisches Institut der Justus-Liebig-Universität Giessen, Giessen, Germany). Percoll® was obtained from Amersham Biosciences. [G-^{3}H]Hypoxanthine (270 GBq/mmol), L-[^{35}S]methionine (>1,000 Ci/mmol), [1-^{14}C]sodium acetate (56 mCi/mmol), and D-[U-^{14}C]glucose (283 mCi/mmol) were obtained from Amersham Biosciences. The chromatographic ion pair, *N′*,*N*-dimethylhexylamine was purchased from Aldrich. The chromatographic ion pair, sodium hexanesulfonate was obtained from Mallinckrodt Baker Inc. All solvents were analytical or HPLC grade.

Parasite Cultures

The experiments were performed with the *P. falciparum* 3D7 clone. Parasites were cultivated according to the method of Trager and Jensen (53) modified by Kimura and colleagues (54). The gas mixture of the tissue culture flasks (75 cm^2) consisted of 5.05% CO_2, 4.93% O_2, and 90.2% N_2. Parasite development and multiplication were monitored by microscopic evaluation of Giemsa-stained thin smears. Ring (1–20 h after reinvasion), trophozoite (20–30 h after reinvasion), and schizont (30–45 h after reinvasion) forms were purified on a 40/70/80% discontinuous Percoll® gradient (10,000 × *g*, 30 min, 25 °C) (55). In the fraction containing the ring stage and uninfected erythrocytes (80%), parasites were isolated by treatment with 0.1% (w/v) saponin for 5 min followed by two washes with phosphate-buffered saline, pH 7.2, at 10,000 × *g* for 10 min. Some experiments were carried out with synchronized parasites in the ring, trophozoite, or schizont stages. Cultures were synchronized by two treatments with 5% (w/v) D-sorbitol solution in water (56).

Inhibition Tests

Fosmidomycin was diluted in culture medium and was used at 5, 2.5, 1.25, 1, 0.75, 0.5, and 0.1 μM concentrations. Inhibition tests were carried out in flat-bottomed microtiter plates (Falcon). The method of Desjardins *et al.* (57) was used to determine the IC_{50} value. Briefly, ring-stage parasite cultures (200 μl per well, with 5% hematocrit and 0.5% parasitemia) were exposed to increasing drug concentrations. After 24 h in culture, [G-^{3}H]hypoxanthine was added (5 μCi/ml final), and after an additional 24-h incubation period, cells were harvested. All tests were done in triplicate. Suspensions of similarly treated, uninfected erythrocytes were used for background determination. Parasitemia and parasite morphology was determined by microscopic analysis of Giemsa-stained blood smears immediately before and at the end of the assays. The IC_{50} value of growth inhibition was calculated using Probit Analysis (Minitab Statistical Software 13.30™, Minitab Inc.).

Metabolic Labeling

The experiments with labeled parasites were performed using two different protocols.

Protocol 1—Asynchronous cultures of *P. falciparum* with ~10% parasitemia untreated or pretreated with 1 μM fosmidomycin for 30 h were labeled for 18 h with [2-^{14}C]DOXP (1.56 μCi/ml), [1-^{14}C]sodium acetate (6.25 μCi/ml), D-[U-^{14}C]glucose (6.25 μCi/ml), or L-[^{35}S]methionine (25 μCi/ml) in the presence of 1 μM fosmidomycin. Radiolabeled amino acid L-[^{35}S]methionine was incorporated into 10 mM methionine-deficient RPMI. For the metabolic labeling with D-[U-^{14}C]glucose all cultures were incubated in glucose-deficient medium (2 g/liter) for 2 h before the addition of the radioactive precursor. Each parasite stage (ring, trophozoite, and schizont) was purified on a discontinuous Percoll® gradient and stored in liquid N_2 for subsequent HPLC analysis. Before being stored or protein-extracted, parasites were separated from red blood cells by incubating with 20 pellet volumes of 0.1% saponin in phosphate-buffered saline, followed by centrifugation (10 min, 10,000 × *g* at 4 °C). For analysis by SDS-PAGE each stage was then purified as described above, followed by lysis of the cells in twice their volume of ice-cold 10 mM Tris-HCl, pH 7.2, 150 mM NaCl, 2% (v/v) Triton X-100, 1 mM phenylmethylsulfonyl fluoride, 5 mM iodoacetamide, 1 mM Na *p*-tosyllysine chloromethyl ketone, and 1 μg/ml leupeptin. After incubation for 15 min at 4 °C, lysates were centrifuged at 10,000 × *g* for 30 min and supernatants were stored in liquid N_2 (54).

Protocol 2—Synchronous cultures of *P. falciparum* starting in ring, trophozoite, or schizont stages with ~10% parasitemia were labeled with [1-^{14}C]sodium acetate (6.25 μCi/ml), and recovered for analysis in

trophozoite, schizont, and ring stages, respectively. The parasites were separated from erythrocytes by treatment with 0.1% (w/v) saponin as described above and stored in liquid N_2 for subsequent HPLC analysis.

Cell Extracts

Each purified parasite stage was freeze-dried and successively extracted with hexane (3× 0.5 ml) and ethanol/water (1:1, v/v; 1× 1 ml at 55 °C for 1.5 h). Aliquots of each extract were monitored for radioactivity with a Beckman LS 5000 TD β-counter.

HPLC

Samples were analyzed using a Gilson HPLC 322 pump (Gilson, Villiers-le-Bel, France) and a gradient module connected to a 152 UV-visible detector, a temperature regulator 831, and a fraction collector FC203B (Gilson, Villiers-le-Bel, France). UNIPOINT™ Software (Gilson Inc.) was used as the operational and analytical system. For comparison of the influence of fosmidomycin treatment on the biosynthesis of the different intermediates, the same quantities of treated or untreated parasites were analyzed. Percent inhibition was determined as follows: [100 − (number of cpm in treated parasites × 100/number of cpm in untreated parasites)].

Identification of DOX and Pyridoxine

The ethanol/water fraction was dephosphorylated with hydrofluoric acid (50%, v/v) for 3 h at room temperature, then neutralized with LiOH and analyzed by HPLC using an Aminex® HPX-87H column (300 × 7.8 cm, Bio-Rad) eluted with 6 mM H_2SO_4 at 65 °C. Standards of pyridoxine and DOX were detected at 190 nm with retention times of 6.75 and 12 min, respectively. The flow rate was 0.6 ml/min. The aliquots were collected at 0.5-min intervals, neutralized with BaOH, and subjected to liquid scintillation counting, or mass spectroscopic analysis in samples without previous labeling (12).

Identification of Pyridoxine

Samples from parasites labeled with [1-^{14}C]sodium acetate were first purified using Aminex® HPX-87H columns as mentioned above. The fractions corresponding to a retention time of 6.75 min were recovered, neutralized, and re-chromatographed by HPLC using an Ultrasphere ODS Beckman column (4.6 mm × 25 cm, 5 μm). The mobile phase was prepared by mixing 25% of methanol with 75% of a 5 mM solution of sodium hexanesulfonate containing 1% (v/v) acetic acid. The flow rate was 0.5 ml/min. The pyridoxine standard was detected at 270 nm with a retention time of 17 min. The aliquots were collected at 1-min intervals and subjected to liquid scintillation counting (58).

Identification of MEP, CDP-ME, CDP-MEP, and ME-2,4-cPP

The ethanol/water fractions were analyzed using an Ultrasphere ODS Beckman column (4.6 mm × 25 cm, 5 μm). The eluents were 20 mM *N*′,*N*-dimethylhexylamine in 10% methanol with the pH was adjusted to 7.0 with formic acid (solvent A) and 50% methanol containing 2 mM *N*′,*N*-dimethylhexylamine, pH 7.0 (solvent B). The HPLC gradient was 10 to 50% methanol in 50 min. The eluent was monitored at 270 nm and the flow rate was 0.75 ml/min. The aliquots were collected at 1-min intervals and subjected to liquid scintillation counting, or ESI-QTOF-MS analysis in unlabeled samples (59).

Analysis of Dolichols

The hexane fraction was analyzed using an Ultrasphere ODS Beckman column (4.6 mm × 25 cm, 5 μm). The gradient elution system used was methanol/water (9:1, v/v; solvent A) and hexane/propan-2-ol/methanol (1:1:2, v/v/v; solvent B). A linear gradient was run from 5 to 100% of B over a period of 25 min. The flow rate was 1.5 ml/min. The eluent was monitored at 210 nm. Fractions were collected at 0.5-min intervals and aliquots were subjected to liquid scintillation counting. Geraniol, geraniolgeraniol, farnesol, dolichol 11, Prenol C_{40-60}, and Prenol C_{80-110} were used as standards and co-injected with the samples (60).

Analysis of Ubiquinones

The hexane fraction was analyzed using an Ultrasphere ODS Beckman column (4.6 mm × 25 cm, 5 μm). Hexane/methanol (75:25, v/v) was used as the solvent system at 1 ml/min flow rate. Standards were detected at 275 nm. One-min fractions were collected and aliquots were monitored for radioactivity. Authentic standards of Q_{7-10} were co-injected with the sample (61).

Mass Spectrometry

The structural characterization of DOX, MEP, CDP-ME, CDP-MEP, and ME-2,4-cPP were accomplished by using 2.5×10^9 parasites obtained from 160 ml of unlabeled asynchronous cultures of *P. falciparum*. The same number of uninfected erythrocytes was analyzed in parallel. Electrospray ionization mass spectrometry (ESI-MS) and tandem mass spectrometry (ESI-MS/MS) were performed with a Finnigan LCQ-Duo ion-trap mass spectrometer (ThermoFinnigan, San Jose, CA). Samples were run in the positive-ion mode with capillary voltage and temperature set at 4.52 kV and 247.8 °C, respectively, in the 50–500 mass-to-charge (*m/z*) range. For ESI-MS/MS analysis a relative collision energy of 30% (1.5 eV) was applied, and the sheath (N_2) and collision helium gas pressures were 1.5 mTorr and 4 p.s.i., respectively. Samples were dissolved in a methanol/water (1:1, v/v), 0.1% formic acid mixture, and analyzed by direct injection using a Harvard Syringe pump model 11 (Harvard Inc., Holliston, MA), operating at 5–10 μl/min flow rate. ESI-QTOF-MS data with high resolution and high mass accuracy were collected in the negative-ion mode using an electrospray ionization hybrid quadrupole orthogonal time-of-flight (TOF) mass spectrometer (Q-TOF, Waters, Micromass Ltd., Manchester, UK) (62, 63). The ESI-QTOF-MS was used for structural characterization of each intermediate of the MEP pathway purified by HPLC. The samples dissolved in a acetonitrile/water (1:1, v/v), 0.1% formic acid mixture were analyzed by direct infusion using a Harvard syringe pump. Typical conditions were: flow rate of 5 μl/min, dissolvation temperature of 100 °C, block temperature of 100 °C, capillary voltage of 3,000 V, and cone voltage of 30 V. The MS experiments were performed by scanning the Q-TOF mass analyzer from 50 to 1,000 *m/z*. In the MS/MS mode, the precursor ion was mass selected by the quadrupole (Q), dissociated by collision with argon in the hexapole collision cell at energies varying from 15 to 45 eV, and the fragment ions formed were then detected by the orthogonal high-resolution TOF mass analyzer. The structural characterization of pyridoxine was accomplished by using 1.8×10^{13} parasites obtained from 240 ml of unlabeled synchronous cultures at the schizont stage. The same number of uninfected erythrocytes was analyzed in parallel. The pellets were extracted with ethanol/water and purified by HPLC using Aminex® HPX-87H column as described above. The ESI-QTOF-MS and MS/MS analyses were carried out as described above, but using the positive-ion mode.

RESULTS

Inhibition of Parasite Development in Cultures of P. falciparum 3D7 Strain Treated with Fosmidomycin—In previous experiments, the IC_{50} of fosmidomycin was determined to be 350, 370, and 290 nM for HB3, A2, and Dd2 strains of *P. falciparum,* respectively (21). To establish the fosmidomycin concentrations at which the 3D7 strain is growth-inhibited but not immediately killed, we first determined the IC_{50} of fosmidomycin in this strain. The IC_{50} value of fosmidomycin was 1.25 ± 0.05 μM for 48 h of treatment. All biosynthesis, experiments were then performed with 1 μM fosmidomycin because under these conditions only a small percentage of parasites died and overall protein synthesis was not affected. Electrophoretic profiles of L-[^{35}S]methionine-labeled proteins from parasites treated or not with fosmidomycin for 48 h were almost the same in the three parasite stages (see Supplemental Materials Fig. data I).

Detection of Biosynthesis of DOXP and Pyridoxine 5′-Phosphate in all Stages of P. falciparum—To characterize the DOXP metabolite, asynchronous cultures were labeled with [1-^{14}C]sodium acetate (see "Experimental Procedures," "Metabolic Labeling, Protocol 1"). Each stage was purified by Percoll® gradients as mentioned above. The first intermediate was analyzed in its dephosphorylated form (DOX) as described in other cellular systems using an HPLC system with an Aminex® HPX-87H column (12). A compound producing a peak with a retention time of 12 min coinciding with the authentic standard of DOX was detected in the three-intraerythrocytic stages of *P. falciparum* (Fig. 1*A*). A similar result was obtained with D-[U-^{14}C]glucose as a metabolic precursor (data not shown). Under identical experimental conditions of metabolic labeling, uninfected erythrocytes did not incorporate or metabolize significant amounts of [1-^{14}C]sodium acetate into mole-

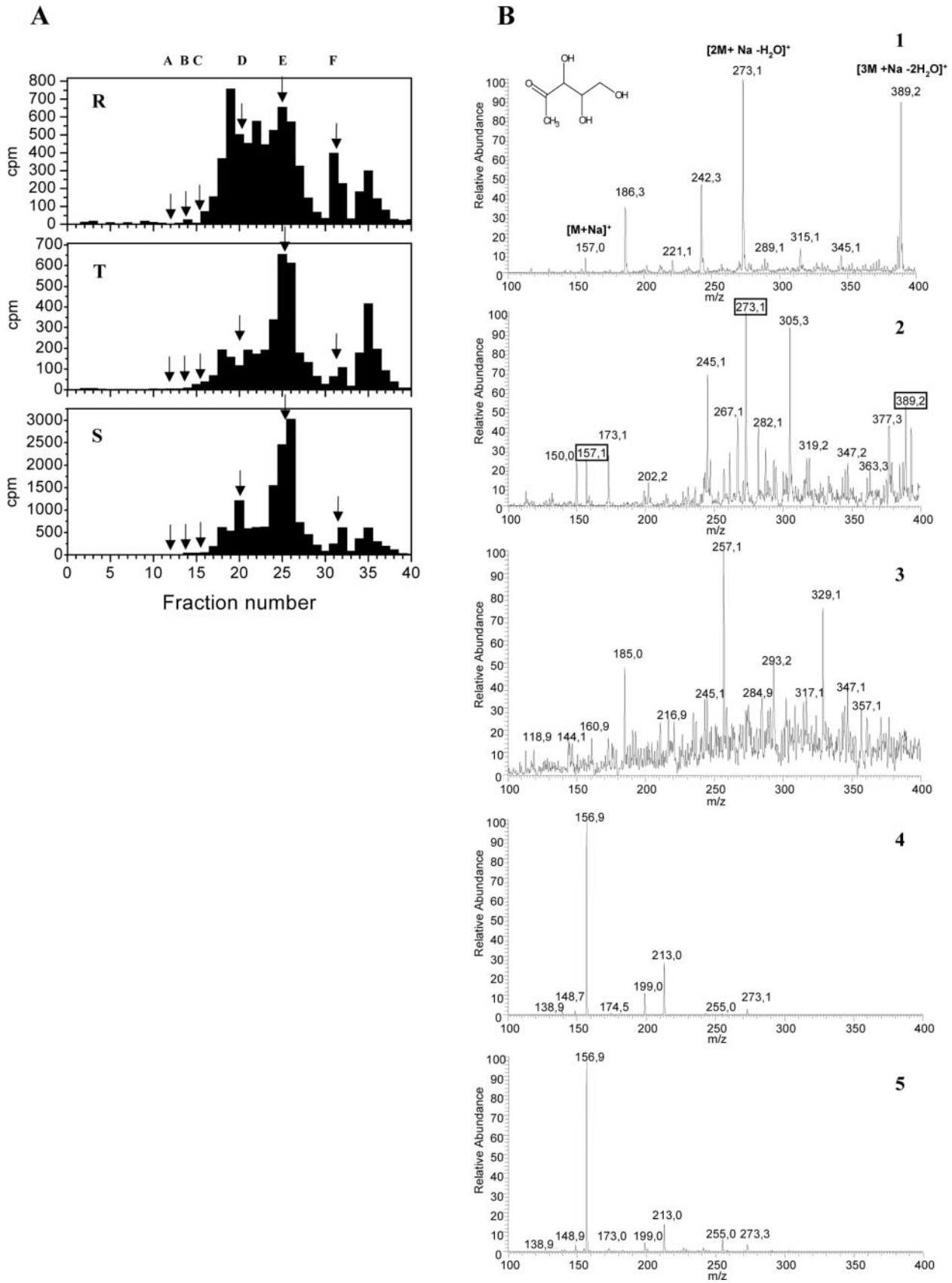

FIG. 1. *A*, radioactive elution profiles of ethanol/water extracts from the different stages of *P. falciparum* metabolically labeled with [1-^{14}C]sodium acetate after HPLC analysis on an Aminex HPX-87H column. Radioactivity in fractions was monitored every 0.5 min. Panels: *R*, ring forms; *T*, trophozoite forms; *S*, schizont forms. *Arrows* indicate the elution positions of authentic standards co-chromatographed in each case: *A*, V_0 and MEP; *B*, DOXP; *C*, pyridoxine; *D*, sodium pyruvate; *E*, DOX; *F*, sodium acetate. *B*, ion trap ESI-MS positive-ion mode analysis of HPLC co-eluted peak E from *P. falciparum* extract (*panel 1*) and authentic DOX (*panel 2*). The *box* indicates the principal ions detected. ESI-MS spectrum of the HPLC co-eluted compounds with DOX standard from the uninfected erythrocyte extract (*panel 3*). Ion trap ESI-MS/MS spectra of the ion of *m/z* 273.1 from *P. falciparum* (*panel 4*) and genuine DOX (*panel 5*), respectively.

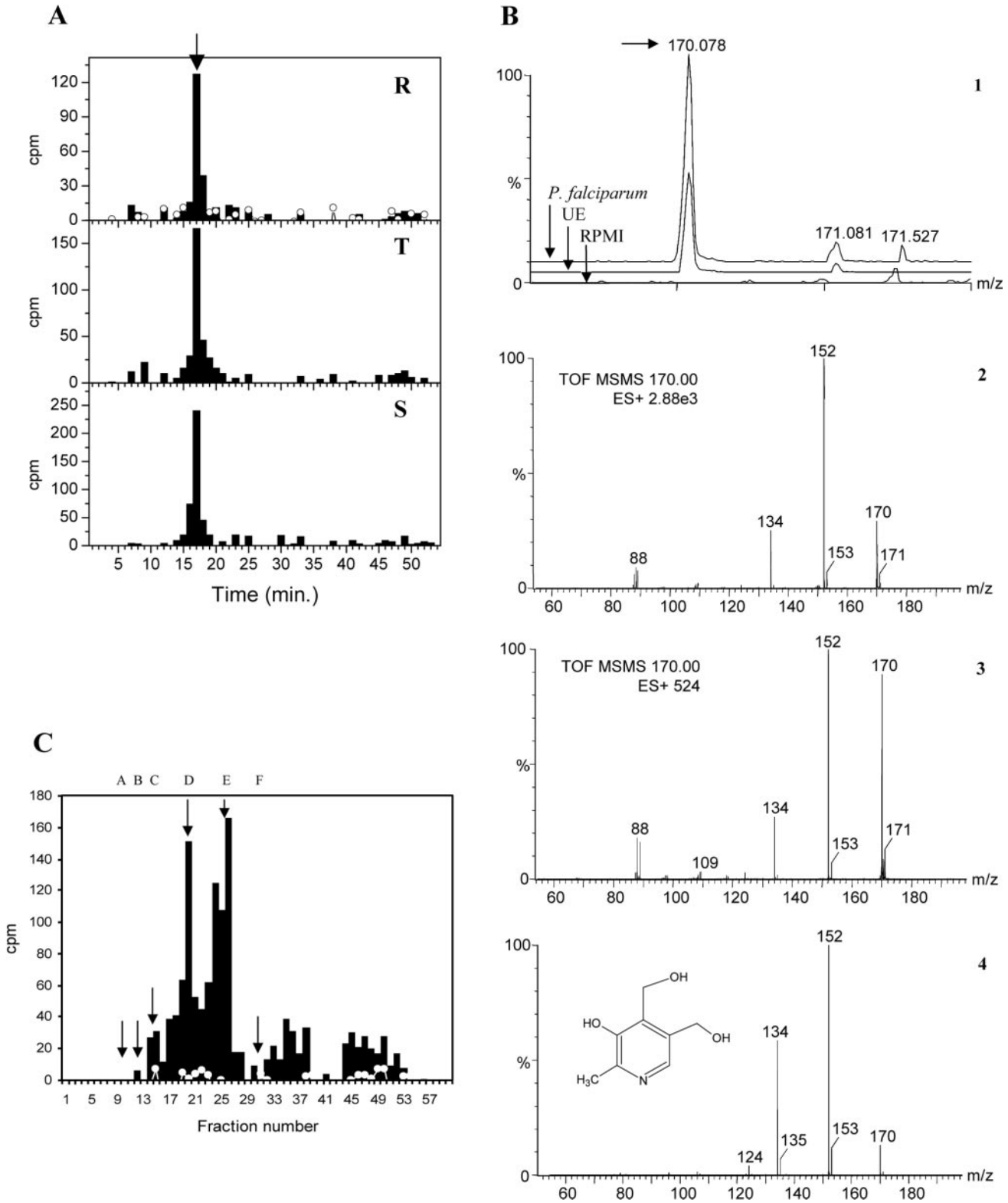

FIG. 2. *A*, radioactive elution profiles of water-soluble metabolites by reverse-phase ion pair HPLC analysis of extracts from different stages of *P. falciparum* metabolically labeled with [1-^{14}C]sodium acetate, pre-purified by the Aminex® HPX-87H column. Panels: *R*, ring forms; *T*, trophozoite forms; *S*, schizont forms. Radioactivity in fractions was monitored at 1-min intervals. *Arrows* indicate the elution position of authentic standards of pyridoxine co-chromatographed in each case. *White circles*, incorporation of labeled precursor into uninfected erythrocytes. *B*, ESI-QTOF-MS positive-ion mode spectra of pyridoxine intermediate purified by HPLC from the schizont stage of *P. falciparum*. *1*, ESI-QTOF-MS spectrum of the compound co-eluting in HPLC with the pyridoxine standard from *P. falciparum* extract, uninfected erythrocytes, and culture medium RPMI. The spectrum of uninfected erythrocyte (*UE*) and *P. falciparum* are shifted 5 and 10% of zero, respectively, for better visualization. *Arrow* indicates the positive-ion corresponding to the mass of pyridoxine. ESI-QTOF-MS/MS profile of the compounds co-eluting in HPLC with pyridoxine from: *2*, parasite extract; *3*, uninfected erythrocytes; *4*, ESI-QTOF-MS/MS for a genuine pyridoxine. The ion intensities of the relative ionization obtained in each MS/MS spectrum from parasite extract and uninfected erythrocytes are indicated. *C*, radioactive separation profile obtained by HPLC analysis of water-soluble metabolites from schizont stages of *P. falciparum* metabolically labeled with [2-^{14}C]DOXP. Radioactivity in fractions was monitored every 0.5 min. *Arrows* indicate the elution positions of authentic standards co-chromatographed as described in the legend to Fig. 1*A*. *White circles*, incorporation of labeled precursor into uninfected erythrocytes.

cules that eluted with the same retention time as seen for the metabolites of interest (data not shown). The compound producing the HPLC peak coinciding with authentic DOX was analyzed by ESI-MS from unlabeled parasite cultures. The positive-ion mode ESI-MS analysis revealed two major singly charged ion species at *m/z* 273.1 and 389.2, which could be assigned to $[2M + Na - H_2O]^+$ and $[3M + Na - 2H_2O]^+$ ions of DOX (monoisotopic molecular mass, 134.1) (Fig. 1*B*, *panel 1*). Also, a minor ion species at *m/z* 157.0, corresponding to a sodiated ion $[M + Na]^+$ of DOX, was observed. These same ion species were detected when the authentic DOX standard was analyzed (Fig. 1*B*, *panel 2*). The MS/MS spectrum for the parasite-derived ion species showed a major fragment ion of *m/z* 156.9 $[M + Na]^+$ (Fig. 1*B*, *panel 4*). A nearly identical dissociation pattern was observed in the MS/MS spectrum of the ion of *m/z* 273.3 from an authentic DOX standard (Fig. 1*B*, *panel 5*). By ESI-MS, the fraction from uninfected erythrocytes co-eluting with the DOX standard showed no significant signals corresponding to DOX ion species (Fig. 1*B*, *panel 3*).

A gene encoding a putative pyridoxine biosynthetic enzyme pdx1 was described in *P. falciparum* (PlasmoDB ID code MAL6P1.215). This gene, in contrast to its *Arabidopsis thaliana* homologue, does not contain any typical apicoplast-targeting signal sequence, but the predicted amino acid sequence shows clearly significant homology to the pdx1 sequence of different organisms. The biochemical analysis for the detection of pyridoxine was performed using the same methodology as described for the detection of DOX. In this system, the pyridoxine is eluted with a retention time of 6.75 min. The pyridoxine was detected in the same samples where DOX was identified. The pyridoxine metabolite was biosynthesized in the three parasite stages from [1-^{14}C]sodium acetate (Fig. 1*A*, *arrow C*). This result was confirmed by the purification of extracts first by an Aminex® HPX-87H column, and a second chromatography in a reverse-phase (C_{18}) ion-pair HPLC system. In this case, only one radioactive compound was detected in fractions co-eluting with the authentic pyridoxine standard. Uninfected erythrocytes did not metabolize [1-^{14}C]sodium acetate into pyridoxine, as expected (Fig. 2*A*). The molecular identity of the fractions corresponding to pyridoxine was determined by ESI-QTOF-MS analysis, confirming the presence of pyridoxine (Fig. 2*B*). The protonated pyridoxine (*m/z* 170.078), under collision-induced dissociation, loses an OH radical, forming the fragment of *m/z* 153 (Scheme 1*A*). The unexpected loss of the OH radical, forming an open shell ion, is favored because the odd electron can be delocalized by the aromatic ring, forming a very stable structure. Alternatively, the protonated pyridoxine (*m/z* 170) loses a neutral H_2O, forming the fragment of *m/z* 152. Both ions, *m/z* 153 and 152, can now lose another water molecule forming the fragment ions of *m/z* 135 and 134, respectively (Scheme 1*A*).

Parasite cultures were labeled with [2-^{14}C]DOXP and analyzed by HPLC. Radioactivity was detected in fractions co-eluting with the authentic pyridoxine standard, confirming that the pathway for *de novo* pyridoxine biosynthesis is metabolically active in *P. falciparum* and that DOXP is indeed the precursor of this metabolite (Fig. 2*C*, *arrow C*). The compounds affording other HPLC peaks found between fractions 32 and 53 were not identified, but they are likely to be sugars or organic acids derived from DOXP or some other downstream metabolites. Uninfected erythrocytes failed to metabolize [2-^{14}C]DOXP (Fig. 2*C*).

Biosynthesis of MEP, CDP-ME, CDP-MEP, and ME-2,4-cPP in Three Intraerythrocytic Stages of P. falciparum—To detect downstream intermediates of DOXP carrying phosphate ester groups, asynchronous cultures were labeled with [1-^{14}C]sodium acetate or [2-^{14}C]DOXP (see "Experimental Procedures," "Metabolic Labeling, Protocol 1"). Each stage was purified by a Percoll® gradient as mentioned above and the extract of ethanol/water was analyzed in a reverse-phase (C_{18}) ion pair HPLC system. In all intraerythrocytic stages of parasites four peaks with retention times coinciding with standards of MEP, CDP-ME, CDP-MEP, and ME-2,4-cPP were detected (Fig. 3). A similar result was obtained with D-[U-^{14}C]glucose as a metabolic precursor (data not shown). The specific precursor [2-^{14}C]DOXP was also metabolized into the four intermediates analyzed (Fig. 3*B*), reproducing the similar profile obtained with [1-^{14}C]sodium acetate (Fig. 3*A*). Under identical experimental conditions of metabolic labeling, uninfected erythrocytes did not incorporate or metabolize significantly [1-^{14}C]sodium acetate into molecules that co-eluted with the metabolites of interest (data not shown). Furthermore, [2-^{14}C]DOXP was not metabolized by uninfected erythrocytes (Fig. 3*B*).

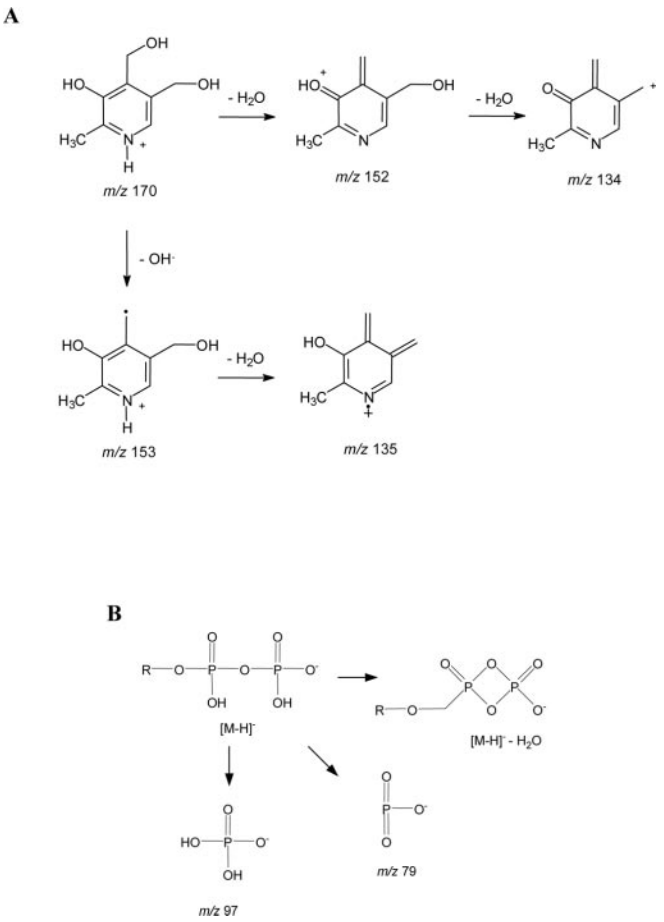

SCHEME 1. *A*, fragmentation pathway of pyridoxine. *B*, phosphate group-driven fragmentation pathway of the phosphorylated compounds.

To confirm that these radioactive compounds correspond to intermediates of the MEP pathway, extracts from unlabeled parasites were purified by ion pair HPLC as described above. The fractions with the same retention time as each standard were then analyzed by ESI-QTOF-MS. The intermediates MEP (monoisotopic molecular mass, 216.126) (Fig. 4*A*, *panel 1*), CDP-ME (monoisotopic molecular mass, 521.308) (Fig. 4*B*, *panel 1*), and ME-2,4-cPP (monoisotopic molecular mass, 278.098) (Fig. 4*C*, *panel 1*) were clearly detected as [M − H] − by negative-ion mode ESI-QTOF-MS. The deprotonated molecules of the MEP, CDP-ME, and ME-2,4-cPP standards were dissociated using 35 eV collision energy (Fig. 4, *A–C*, *panel 3*), showing a dissociation mostly driven by the phosphate group as

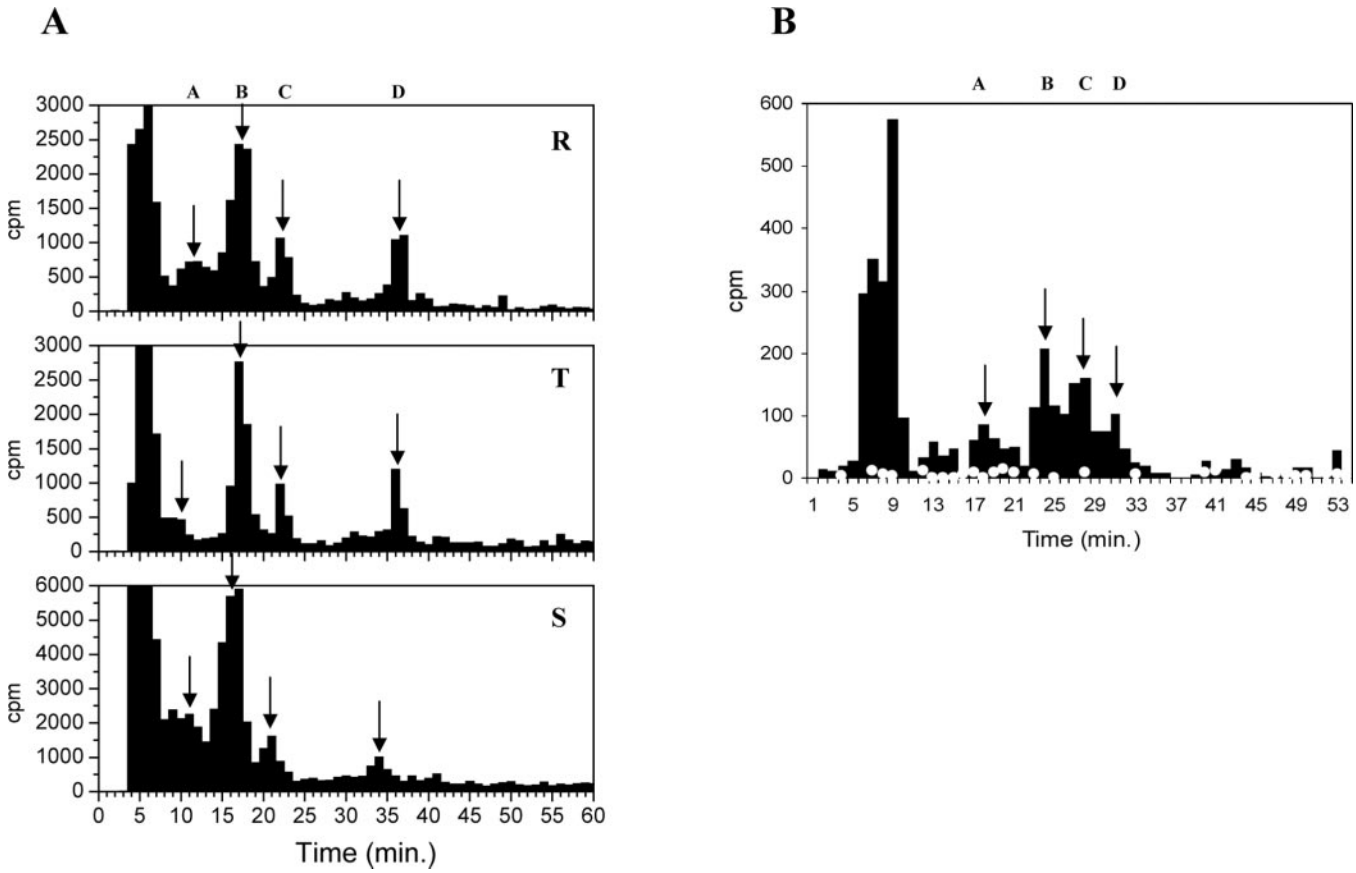

FIG. 3. **Radioactive elution profiles of water-soluble metabolites derived from different stages of *P. falciparum* metabolically labeled with (*A*) [1-^{14}C]sodium acetate or (*B*) [2-^{14}C]DOXP after reverse-phase ion-pair HPLC analysis.** Radioactivity in fractions was monitored at 1-min intervals. Panels: *R*, ring forms; *T*, trophozoite forms; *S*, schizont forms. *Arrows* indicate the elution positions of authentic standards co-chromatographed in each case: *A*, MEP; *B*, CDP-ME; *C*, ME-2,4-cPP; *D*, CDP-MEP. *White circles*, incorporation of labeled precursor into uninfected erythrocytes.

shown in Scheme 1*B*. Under the same conditions, the MS/MS spectrum of deprotonated MEP, CDP-ME, and ME-2,4-cPP from parasites displayed the same ionic fragments, confirming their identities (Fig. 4, *A–C*, *panel 4*). The fractions from uninfected erythrocytes with the same retention time of each of the standards analyzed were purified. These fractions failed to show any significant ions by ESI-QTOF-MS (Fig. 4, *A–C*, *panel 2*). The intermediate CDP-MEP was not detected by ESI-QTOF-MS probably because the amount was too low. However, the presence of this metabolite was confirmed by specific labeling with [2-^{14}C]DOXP (Fig. 3*B*).

To confirm that all intermediates analyzed are biosynthesized in a continuous form in the three stages of the parasite, synchronous cultures of *P. falciparum* were labeled with [1-^{14}C]sodium acetate (see "Experimental Procedures," "Metabolic Labeling, Protocol 2"). Each stage was analyzed by HPLC and ESI-QTOF-MS as described above. We detected active biosynthesis of DOXP, MEP, CDP-ME, CDP-MEP, and ME-2,4-cPP in the ring, trophozoite, and schizont stages (data not shown).

Effect of Fosmidomycin on the Biosynthesis of DOXP, Pyridoxine 5′-Phosphate, MEP, CDP-ME, CDP-MEP, and ME-2,4-cPP in Intraerythrocytic Stages of P. falciparum—The effect of fosmidomycin on the biosynthesis of the different intermediates of the MEP pathway was also evaluated by HPLC analysis. The same numbers of treated and untreated parasites for each stage were injected into the HPLC system. The experiment was repeated three times with comparable results and the results of a typical experiment are shown in Table I. When asynchronous cultures were treated with 1 μM fosmidomycin for 48 h and labeled with [1-^{14}C]sodium acetate in the last 18 h (see "Experimental Procedures," "Metabolic Labeling, Protocol 1") the biosynthesis of DOXP showed a low inhibition of 4 and 3% in ring and trophozoite stages, respectively. However, in schizont stages a 26% increase in DOXP detection was found (Table I). The biosynthesis of pyridoxine 5′-phosphate was increased by 42 and 33% in the trophozoite and schizont stages, respectively, but in the ring stage fosmidomycin exerted no effect on this metabolite (Table I). As expected, the biosynthesis of MEP, CDP-ME, CDP-MEP, and ME-2,4-cPP was inhibited 46 to 67% in fosmidomycin-treated ring stages. Low levels of inhibition were detected in the biosynthesis of these products in trophozoite stages, whereas in schizont stages the biosynthesis was diminished 20–40%, except for ME-2,4-cPP, which was not influenced (Table I).

Effect of Fosmidomycin on Biosynthesis of Dolichols and Ubiquinones—The biosynthesis of dolichols and ubiquinones depends on an active IPP and DMPP synthesis. To analyze the effect of fosmidomycin on these pathways, asynchronous cultures were treated with 1 μM antibiotic and labeled with [1-^{14}C]sodium acetate as described (see "Experimental Procedures," "Metabolic Labeling, Protocol 1"). Each stage was purified by Percoll® gradient as described above and the hexane extracts were analyzed by HPLC. Equal quantities of treated or untreated parasites were analyzed. Biosynthesis of dolichol was inhibited with fosmidomycin in ring (91%) and schizont stages (35%). In trophozoite stages no effect on the dolichol biosynthesis was detected.

When the ubiquinone biosynthesis was analyzed in parasites treated with fosmidomycin the highest inhibition was detected

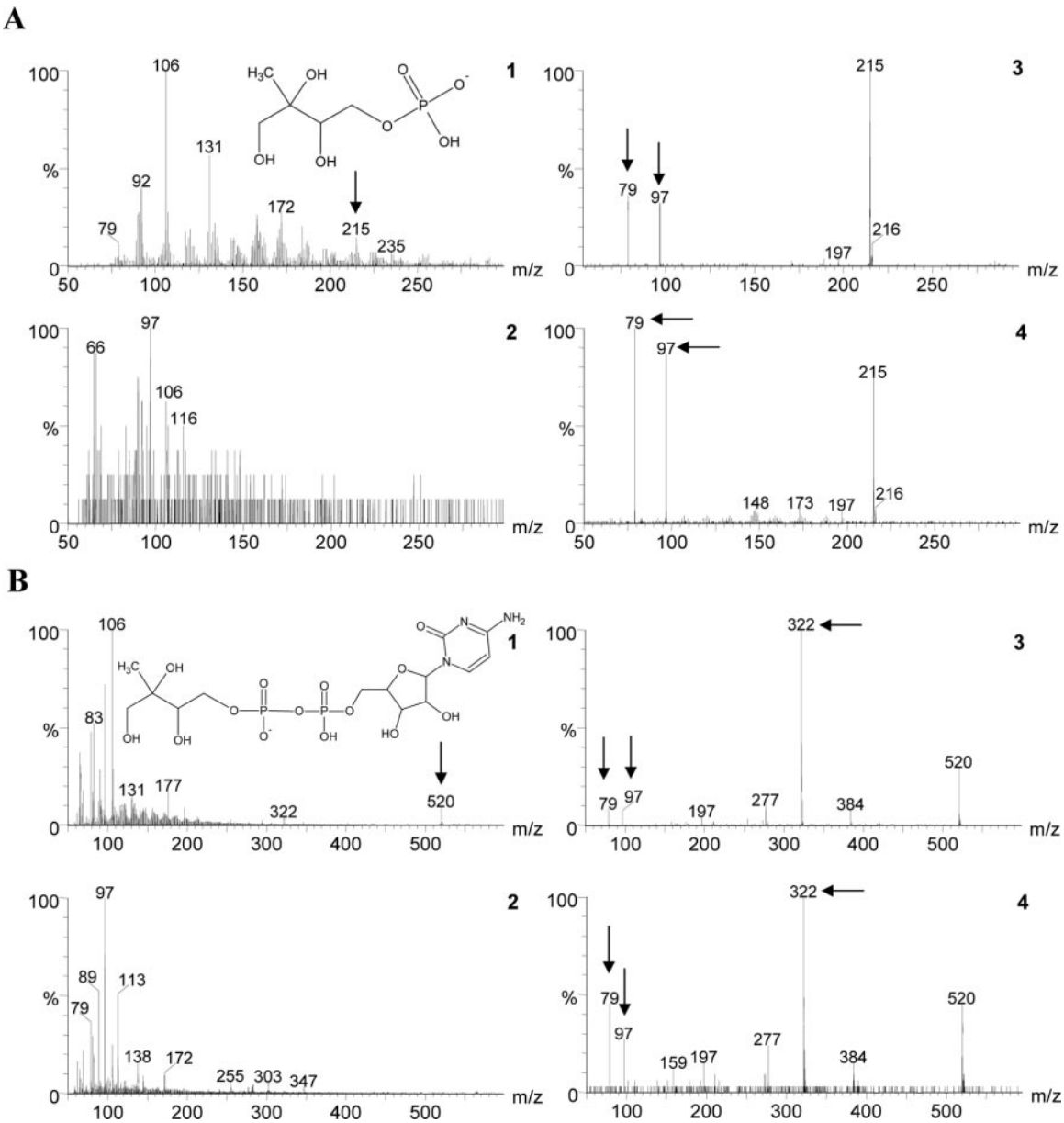

FIG. 4. **ESI-QTOF-MS negative-ion mode spectra of MEP, CDP-ME, and ME-2,4-cPP intermediates purified by HPLC from the schizont stage of *P. falciparum*.** *Arrows* indicate the major ions detected. *A*, ESI-QTOF-MS spectrum of the compounds co-eluting in HPLC with the MEP standard from: *1*, *P. falciparum* extract and *2*, uninfected erythrocytes; and ESI-QTOF-MS/MS spectrum of the intermediate from: *3*, genuine MEP and *4*, *P. falciparum* extract co-eluting with MEP. *B*, ESI-QTOF-MS profile of the compounds co-eluting in HPLC with CDP-ME from: *1*, parasite extract and *2*, uninfected erythrocytes; and ESI-QTOF-MS/MS for CDP-ME from: *3*, genuine CDP-ME and *4*, *P. falciparum* extract after HPLC purification. *C*, ESI-QTOF-MS spectrum for the peak constituents purified by HPLC with the same retention time as ME-2,4-cPP standard from: *1*, parasites extract and *2*, uninfected erythrocytes; and ESI-QTOF-MS/MS from: *3*, genuine ME-2,4-cPP and *4*, the intermediate ME-2,4-cPP from *P. falciparum* extract after HPLC purification.

in ring stages (about 95%). Percent inhibition was around 23% in trophozoite stages and 13% in schizont stages (Table I).

DISCUSSION

In this study, we demonstrate the metabolites of the biochemical pathway of plastid MEP biosynthesis in *P. falciparum,* which was so far fully assembled *in silico* by Ralph and colleagues (64). We have isolated and characterized the MEP pathway metabolites DOXP, MEP, CDP-ME, CDP-MEP, and ME-2,4-cPP by different methods. We have also shown the active *de novo* biosynthesis of pyridoxine 5′-phosphate in *P. falciparum.* This is the first demonstration of pyridoxine 5′-phosphate biosynthesis in parasitic protozoa. Both pathways are active in the ring, trophozoite, and schizont stages. So far, all genes related to the MEP pathway were identified in the *P. falciparum* genome but only three genes that encode the enzymes 1-deoxy-D-xylulose-5-phosphate synthase, 1-deoxy-D-xylulose-5-phosphate reductoisomerase, and 2-*C*-methyl-D-erythritol-2,4-cyclodiphosphate synthase were functionally characterized.

All but one of the intermediates of the MEP pathway were detected and characterized by two independent methods, also recently employed for the detection of these metabolites in the chromoplasts of higher plants (65). To achieve efficient labeling, [1-^{14}C]sodium acetate and D-[U-^{14}C]glucose were employed instead of pyruvic acid, which is not incorporated by blood stage *P. falciparum* (66, 67).

The DOXP metabolite is not only an intermediate for IPP and dimethylallyl diphosphate biosynthesis but is also involved

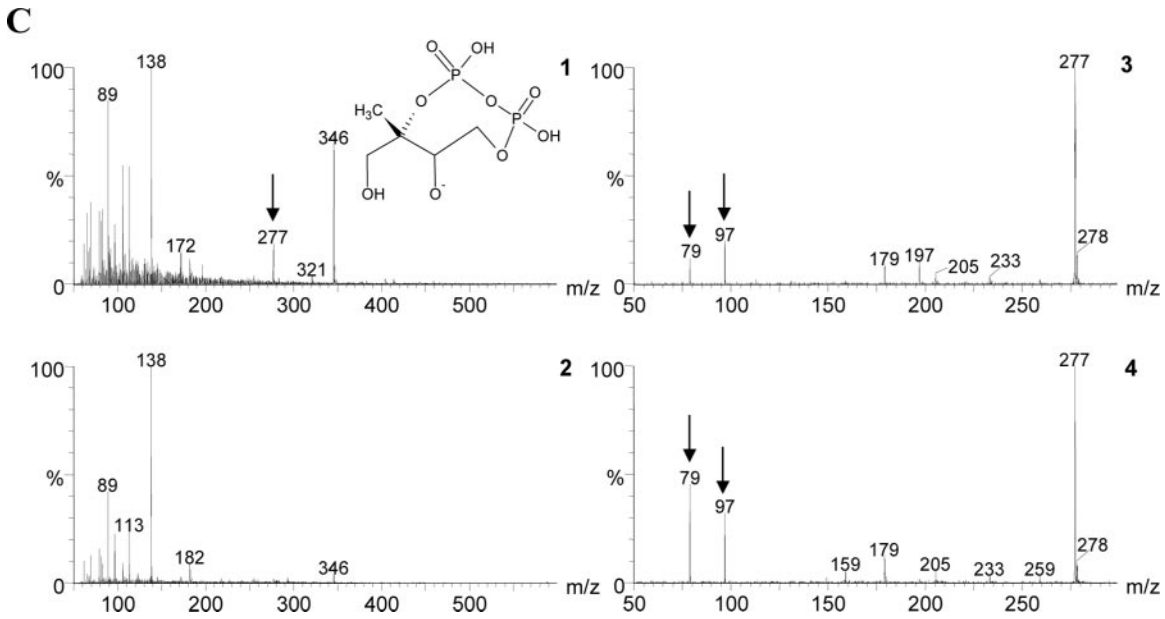

FIG. 4—*continued*

TABLE I

Effect of fosmidomycin on the biosynthesis of pyridoxine 5′-phosphate, DOXP, downstream intermediates of the MEP pathway, dolichols and ubiquinones in parasites metabolically labeled with [1-^{14}C]sodium acetate

Each experiment was done in triplicate and standard deviations are indicated in parentheses. The effect of fosmidomycin on each intermediate was analyzed as the relationship between control and fosmidomycin-treated parasites. The positive values indicate accumulation of the intermediate and negative values indicate reduction of the intermediate biosynthesis.

Metabolite analyzed	Control	Fosmidomycin	Effect
	cpm		*%*
Ring			
Pyridoxine 5′-P[a]	109 (15)	131 (17)	0
DOXP[a]	2125 (91)	1875 (79)	−4
MEP	336 (35)	142 (22)	−46
CDP-ME	1177 (52)	458 (43)	−55
CDP-MEP	1659 (72)	484 (45)	−67
ME-2,4-cPP	3696 (137)	1602 (72)	−53
Ubiquinones	4800 (120)	194 (27)	−95
Dolichols	522 (43)	39 (5)	−91
Trophozoite			
Pyridoxine 5′-P[a]	66 (10)	127 (19)	+42
DOXP[a]	2863 (116)	2566 (110)	−3
MEP	886 (52)	843 (53)	0
CDP-ME	5040 (140)	3652 (137)	−23
CDP-MEP	382 (35)	302 (32)	−4
ME-2,4-cPP	532 (52)	621 (51)	0
Ubiquinones	1147 (49)	787 (54)	−23
Dolichols	122 (19)	130 (19)	0
Schizont			
Pyridoxine 5′-P[a]	198 (25)	328 (32)	+33
DOXP[a]	12641 (220)	16446 (248)	+26
MEP	2138 (93)	1571 (56)	−20
CDP-ME	25654 (310)	18558 (290)	−26
CDP-MEP	1060 (52)	551 (53)	−40
ME-2,4-cPP	2153 (94)	2021 (94)	0
Ubiquinones	3073 (115)	2465 (98)	−13
Dolichols	718 (50)	393 (39)	−35

[a] Values obtained from fractions analyzed as DOX and pyridoxine.

in the biosynthesis of thiamin and pyridoxine (39–42). The organisms that are unable to carry out the *de novo* synthesis of vitamin B_6 do need to obtain the vitamers (pyridoxal, pyridoxamine, and pyridoxine) through the diet. Pyridoxal 5′-phosphate, the active form of vitamin B_6, is an essential co-factor of many enzymes in the metabolic transformation of amino acids in humans, animals, plants, and microorganisms, and probably also in the malaria parasite. *P. falciparum* has a gene encoding a putative pyridoxine biosynthetic enzyme (*pdx1*), which has homology with genes found in plants, fungi, archaebacteria, and a subset of eubacteria, but lacks homology with *E. coli* (43). We detected pyridoxine 5′-phosphate in *P. falciparum* after metabolic labeling with [1-^{14}C]sodium acetate and [2-^{14}C]DOXP by HPLC analysis in the three stages of the parasite. The herein described method using Aminex® HPX-87H columns has never been used for the analysis of pyridoxine. To validate the presence of this compound we re-chromatographed the fractions recovered from this column in a specific system described for this metabolite (Fig. 2*A*). We detected only one radioactive peak coincident with the authentic standard of pyridoxine. The subsequent molecular identification of pyridoxine in the fractions purified by the Aminex® HPX-87H column was performed by ESI-QTOF-MS analysis in schizont stages. The MS/MS (collision induced dissociation) spectrum of pyridoxine from parasites and uninfected erythrocytes displayed the same ionic fragments as the authentic standard, confirming their identities. Additionally, both the MS and MS/MS spectrum of pyridoxine from parasites and uninfected erythrocytes showed a significant difference in the relative quantity of detected ions (2- and 5-fold greater in the MS and MS/MS spectra in the parasite sample, respectively). These results indicate that the difference is because of the *de novo* biosynthesis of the parasite. Importantly, the culture medium does not contain pyridoxine (Fig. 2*B*, *panel 1*). The detection of pyridoxine by HPLC in parasites, but not in uninfected red blood cells when labeled with [2-^{14}C]DOXP, confirms that this metabolite is indeed produced by *P. falciparum* (Fig. 2*C*, *arrow C*). Additionally, the levels of pyridoxine measured by incorporation of [1-^{14}C]sodium acetate were increased when the parasites were treated with fosmidomycin, suggesting that when DOXP cannot be metabolized to MEP by inhibition of DOXP reductoisomerase, the biosynthesis of pyridoxine might be stimulated (Table I).

All the MEP pathway-associated enzymes contain an apicoplast-targeting signal, which strongly supports the idea that the pathway is indeed localized in the apicoplast (64). Noteworthy, the best candidate gene for the synthesis of pyridoxal has no apicoplast-targeting signal, which means that the substrate DOXP is exported from the apicoplast. However, unlike *pdx1*,

there is no gene homologue to *pdx2* predicted in the *P. falciparum* genome. Pdx2 proteins are less conserved than pdx1 but contain several motifs that are conserved (68). We found a potential gene (PlasmoDB ID code PF11_0169) with conserved domains also present in pdx2 (see Supplemental Materials Fig. data II) (69).

Downstream intermediates of DOXP, *i.e.* MEP, CDP-ME, CDP-MEP, and ME-2,4-cPP, were detected in the three stages after metabolic labeling with both [2-^{14}C]DOXP and [1-^{14}C]sodium acetate, followed by reverse-phase ion pair HPLC analysis. The presence of MEP, CDP-ME, and ME-2,4-cPP was confirmed by ESI-QTOF-MS analysis in schizont stages. We were unable to detect CDP-MEP by ESI-QTOF-MS, probably because of the higher detection limit of this experimental system as compared with radioactive analysis. The cutoff for biomolecule detection is of the order of 10^{-15} molar in ESI-QTOF-MS analysis, and of 10^{-18} molar in radioactivity analysis. A similar result was described in chromoplasts of higher plants (65). By the same experimental approach, but using synchronous cultures we also detected the MEP pathway intermediates, suggesting that the pathway is continuously active throughout the blood stage form.

1-Deoxy-D-xylulose-5-phosphate reductoisomerase catalyzes the simultaneous intramolecular rearrangement and reduction of DOXP to form MEP (18–22) and the activity of this enzyme is specifically inhibited by fosmidomycin (23). We analyzed the effect of treatment with fosmidomycin on the downstream DOXP intermediates MEP, CDP-ME, CDP-MEP, and ME-2,4-cPP in the ring, trophozoite, and schizont stages. As expected, these metabolites were inhibited in all phases but the effect was more evident at the ring stage (Table I). On the other hand, it has been described in plants that the MEP intermediate is used for the biosynthesis of other metabolites such as 2-*C*-methyl-D-erythronolactone (70), glycosides (71), and ADP-ME (65). Because *P. falciparum* is metabolically very similar to plants regarding the presence of apicoplasts, it is possible that the parasites use the MEP intermediate to synthesize other products, as observed in plants. These hypotheses are currently being tested in our laboratory.

The isoprenic units synthesized by the MEP pathway are used not only for the modification of tRNAs that are essential for apicoplast translation, but also for extraplastidic compounds such as ubiquinones and dolichol biosynthesis (60, 61, 64). The biosynthesis of ubiquinone and dolichol were also inhibited by treatment with fosmidomycin suggesting that the precursors for these isoprenoids are biosynthesized by the MEP pathway. The inhibition was more evident in ring and schizont stages.

Finally, the patterns of proteins labeled with L-[^{35}S]methionine were similar for parasites treated or not with fosmidomycin. Therefore, we suggest that the effect of fosmidomycin on the biosynthesis of DOXP and its derivatives as well as dolichols and the isoprenic chain attached to ubiquinones was specific.

Several hypotheses could be suggested to explain the low level of inhibition of the biosynthesis of MEP, CDP-ME, CDP-MEP, ME-2,4-cPP, dolichols, and the isoprenic chain of ubiquinones detected in trophozoite and schizont stages obtained from asynchronous cultures treated with fosmidomycin: (*a*) an alternative pathway for the biosynthesis of IPP and dimethylallyl diphosphate could be active in which xylulose 5′-phosphate is considered as a precursor (72, 73); and (*b*) if *P. falciparum* performs active *de novo* biosynthesis of thiamin from DOXP, the levels of thiamin diphosphate could be increased in fosmidomycin-treated parasites, as we demonstrated for pyridoxine 5′-phosphate. Because 1-deoxy-D-xylulose-5-phosphate synthase is thiamin diphosphate-dependent, its enzymatic activity could be modulated and, as a consequence, the downstream enzymes from the MEP pathway, too. In fact, *P. falciparum* possibility synthesizes thiamin because three genes involved in the *de novo* thiamin biosynthesis were found in the parasite genome (PlasmoDB ID codes PF13_0344, PFE1030c and MAL6P1.285). Both hypotheses are currently being tested in our laboratory.

Taken together, the chemical identification of all but one intermediate of a pathway not present in humans and the identification of the active *de novo* synthesis of pyridoxine opens new possibilities to block parasite development. Both pathways are present in several human pathogens and this fact makes these pathways interesting chemotherapeutic targets.

Acknowledgments—We thank Renata Tonhosolo and Herbert Rodrigues Goulart for technical assistance and stimulating discussions of the results.

REFERENCES

1. Moore, S. A., Surgey, E. G., and Cadwgan, A. M. (2002) *Lancet Infect. Dis.* **2,** 737–743
2. Fevre, E. M., and Barnish, G. (1999) *Ann. Trop. Med. Parasitol.* **93,** 549–560
3. Aubouy, A., Bakary, M., Keundjian, A., Mbomat, B., Makita, J. R., Migot-Nabias, F., Cot, M., Le Bras, J., and Deloron, P. (2003) *Antimicrob. Agents Chemother.* **47,** 231–237
4. Goldstein, J. L., and Brown, M. S. (1990) *Nature* **343,** 425–430
5. Lichtenthaler, H. K. (1999) *Annu. Rev. Plant Physiol. Plant Mol. Biol.* **50,** 47–65
6. Lichtenthaler, H. K., Rohmer, M., and Schwender, J. (1997) *Physiol. Plant.* **101,** 643
7. Eisenreich, W., Schwarz, M., Cartayrade, A., Arigoni, D., Zenk, M. H., and Bacher, A. (1998) *Chem. Biol.* **5,** R221–R233
8. Eisenreich, W., Rohdich, F., and Bacher, A. (2001) *Trends Plant Sci.* **6,** 78–84
9. Rohmer, M. (1999) *Nat. Prod. Rep.* **16,** 565–574
10. Rodriguez-Concepcion, M., and Boronat, A. (2002) *Plant Physiol.* **130,** 1079–1089
11. Rohmer, M., Knani, M., Simonin, P., Sutter, B., and Sahm, H. (1993) *Biochem. J.* **295,** 517–524
12. Sprenger, G. A., Schorken, U., Wiegert, T., Grolle, S., de Graaf, A. A., Taylor, S. V., Begley, T. P., Bringer-Meyer, S., and Sahm, H. (1997) *Proc. Natl. Acad. Sci. U. S. A.* **94,** 12857–12862
13. Bouvier, F., d'Harlingue, A., Suire, C., Backhaus, R. A., and Camara, B. (1998) *Plant Physiol.* **117,** 1423–1431
14. Lange, B. M., Wildung, M. R., McCaskill, D., and Croteau, R. (1998) *Proc. Natl. Acad. Sci. U. S. A.* **95,** 2100–2104
15. Lois, L. M., Campos, N., Putra, S. R., Danielsen, K., Rohmer, M., and Boronat, A. (1998) *Proc. Natl. Acad. Sci. U. S. A.* **95,** 2105–2110
16. Kuzuyama, T., Takagi, M., Takahashi, S., and Seto, H. (2000) *J. Bacteriol.* **182,** 891–897
17. Flesch, G., and Rohmer, M. (1988) *Eur. J. Biochem.* **175,** 405–411
18. Kuzuyama, T., Takahashi, S., Watanabe, H., and Seto, H. (1998) *Tetrahedron Lett.* **39,** 4509–4512
19. Takahashi, S., Kuzuyama, T., Watanabe, H., and Seto, H. (1998) *Proc. Natl. Acad. Sci. U. S. A.* **95,** 9879–9884
20. Lange, B. M., and Croteau, R. (1999) *Arch. Biochem. Biophys.* **365,** 170–174
21. Jomaa, H., Wiesner, J., Sanderbrand, S., Altincicek, B., Weidemeyer, C., Hintz, M., Turbachova, I., Eberl, M., Zeidler, J., Lichtenthaler, H. K., Soldati, D., and Beck, E. (1999) *Science* **285,** 1573–1576
22. Schwender, J., Muller, C., Zeidler, J., and Lichtenthaler, H. K. (1999) *FEBS Lett.* **455,** 140–144
23. Kuzuyama, T., Shimizu, T., Takahashi, S., and Seto, H. (1998) *Tetrahedron Lett.* **39,** 7913–7916
24. Rohdich, F., Wungsintaweekul, J., Fellermeier, M., Sagner, S., Herz, S., Kis, K., Eisenreich, W., Bacher, A., and Zenk, M. H. (1999) *Proc. Natl. Acad. Sci. U. S. A.* **96,** 11758–11763
25. Herz, S., Wungsintaweekul, J., Schuhr, C. A., Hecht, S., Luttgen, H., Sagner, S., Fellermeier, M., Eisenreich, W., Zenk, M. H., Bacher, A., and Rohdich, F. (2000) *Proc. Natl. Acad. Sci. U. S. A.* **97,** 2486–2490
26. Luttgen, H., Rohdich, F., Herz, S., Wungsintaweekul, J., Hecht, S., Schuhr, C. A., Fellermeier, M., Sagner, S., Zenk, M. H., Bacher, A., and Eisenreich, W. (2000) *Proc. Natl. Acad. Sci. U. S. A.* **97,** 1062–1067
27. Hintz, M., Reichenberg, A., Altincicek, B., Bahr, U., Gschwind, R. M., Kollas, A. K., Beck, E., Wiesner, J., Eberl, M., and Jomaa, H. (2001) *FEBS Lett.* **509,** 317–322
28. Hecht, S., Eisenreich, W., Adam, P., Amslinger, S., Kis, K., Bacher, A., Arigoni, D., and Rohdich, F. (2001) *Proc. Natl. Acad. Sci. U. S. A.* **98,** 14837–14842
29. Rohdich, F., Hecht, S., Gartner, K., Adam, P., Krieger, C., Amslinger, S., Arigoni, D., Bacher, A., and Eisenreich, W. (2002) *Proc. Natl. Acad. Sci. U. S. A.* **99,** 1158–1163
30. Adam, P., Hecht, S., Eisenreich, W., Kaiser, J., Grawert, T., Arigoni, D., Bacher, A., and Rohdich, F. (2002) *Proc. Natl. Acad. Sci. U. S. A.* **99,** 12108–12113
31. Wolff, M., Seemann, M., Grosdemange-Billiard, C., Tritsch, D., Campos, N., Rodríguez-Concepción, M., Boronat, A., and Rohmer, M. (2002) *Tetrahedron Lett.* **43,** 2555–2559
32. Giner, J. L., Jaun, B., and Arigoni, D. (1998) *Chem. Commun.* 1857–1858

33. Sacchettini, J. C., and Poulter, C. D. (1997) *Science* **277,** 1788–1789
34. Barkovich, R., and Liao, J. C. (2001) *Metab. Eng.* **3,** 27–39
35. Sinensky, M. (2000) *Biochim. Biophys. Acta* **1484,** 93–106
36. Lell, B., Ruangweerayut, R., Wiesner, J., Missinou, M. A., Schindler, A., Baranek, T., Hintz, M., Hutchinson, D., Jomaa, H., and Kremsner, P. G. (2003) *Antimicrob. Agents Chemother.* **47,** 735–738
37. Wiesner, J., Henschker, D., Hutchinson, D. B., Beck, E., and Jomaa, H. (2002) *Antimicrob. Agents Chemother.* **46,** 2889–2894
38. Rohdich, F., Eisenreich, W., Wungsintaweekul, J., Hecht, S., Schuhr, C. A., and Bacher, A. (2001) *Eur. J. Biochem.* **268,** 3190–3197
39. White, R. H. (1978) *Biochemistry* **17,** 3833–3840
40. Hill, R. E., Himmeldirk, K., Kennedy, I. A., Pauloski, R. M., Sayer, B. G., Wolf, E., and Spenser, I. D. (1996) *J. Biol. Chem.* **271,** 30426–30435
41. Cane, D. E., Du, S., Robinson, J. K., Hsiung, Y., and Spenser, I. D. (1999) *J. Am. Chem. Soc.* **121,** 7722–7723
42. Cane, D. E., Du, S., and Spenser, I. D. (2000) *J. Am. Chem. Soc.* **122,** 4213–4214
43. Ehrenshaft, M., Bilski, P., Li, M. Y., Chignell, C. F., and Daub, M. E. (1999) *Proc. Natl. Acad. Sci. U. S. A.* **96,** 9374–9378
44. Osmani, A. H., May, G. S., and Osmani, S. A. (1999) *J. Biol. Chem.* **274,** 23565–23569
45. Lam, H. M., Tancula, E., Dempsey, W. B., and Winkler, M. E. (1992) *J. Bacteriol.* **174,** 1554–1567
46. Roa, B. B., Connolly, D. M., and Winkler, M. E. (1989) *J. Bacteriol.* **171,** 4767–4777
47. Lam, H. M., and Winkler, M. E. (1992) *J. Bacteriol.* **174,** 6033–6045
48. Lam, H. M., and Winkler, M. E. (1990) *J. Bacteriol.* **172,** 6518–6528
49. Galperin, M. Y., and Koonin, E. V. (1997) *Mol. Microbiol.* **24,** 443–445
50. Bauer, J. A., Bennett, E. M., Begley, T. P., and Ealick, S. E. (2004) *J. Biol. Chem.* **279,** 2704–2711
51. Wetzel, D. K., Ehrenshaft, M., Denslow, S. A., and Daub, M. E. (2004) *FEBS Lett.* **564,** 143–146
52. Okamoto, T., Fukui, K., Nakamoto, M., Kishi, T., Okishio, T., Yamagami, T., Kanamori, N., Kishi, H., and Hiraoka, E. (1985) *J. Chromatogr.* **342,** 35–46
53. Trager, W., and Jensen, J. B. (1976) *Science* **193,** 673–675
54. Kimura, E. A., Couto, A. S., Peres, V. J., Casal, O. L., and Katzin, A. M. (1996) *J. Biol. Chem.* **271,** 14452–14461
55. Braun-Breton, C., Jendoubi, M., Brunet, E., Perrin, L., Scaife, J., and Pereira da Silva, L. (1986) *Mol. Biochem. Parasitol* **20,** 33–43
56. Lambros, C., and Vanderberg, J. P. (1979) *J. Parasitol.* **65,** 418–420
57. Desjardins, R. E., Canfield, C. J., Haynes, J. D., and Chulay, J. D. (1979) *Antimicrob. Agents Chemother.* **16,** 710–718
58. Kirchmeier, R. L., and Upton, R. P. (1978) *J. Pharmacol. Sci.* **67,** 1444–1446
59. Monkkonen, H., Moilanen, P., Monkkonen, J., Frith, J. C., Rogers, M. J., and Auriola, S. (2000) *J. Chromatogr. B Biomed. Sci. Appl.* **738,** 395–403
60. Couto, A. S., Kimura, E. A., Peres, V. J., Uhrig, M. L., and Katzin, A. M. (1999) *Biochem. J.* **341,** 629–637
61. de Macedo, C. S., Uhrig, M. L., Kimura, E. A., and Katzin, A. M. (2002) *FEMS Microbiol. Lett.* **207,** 13–20
62. Sabino, A. A., Machado, A. H., Correia, C. R., and Eberlin, M. N. (2004) *Angew. Chem. Int. Ed. Engl.* **43,** 2514–2518
63. Rioli, V., Gozzo, F. C., Heimann, A. S., Linardi, A., Krieger, J. E., Shida, C. S., Almeida, P. C., Hyslop, S., Eberlin, M. N., and Ferro, E. S. (2003) *J. Biol. Chem.* **278,** 8547–8555
64. Ralph, S. A., Van Dooren, G. G., Waller, R. F., Crawford, M. J., Fraunholz, M. J., Foth, B. J., Tonkin, C. J., Roos, D. S., and McFadden, G. I. (2004) *Nat. Rev. Microbiol.* **2,** 203–216
65. Fellermeier, M., Sagner, S., Spiteller, P., Spiteller, M., and Zenk, M. H. (2003) *Phytochemistry* **64,** 199–207
66. Elliott, J. L., Saliba, K. J., and Kirk, K. (2001) *Biochem. J.* **355,** 733–739
67. Cranmer, S. L., Conant, A. R., Gutteridge, W. E., and Halestrap, A. P. (1995) *J. Biol. Chem.* **270,** 15045–15052
68. Ehrenshaft, M., and Daub, M. E. (2001) *J. Bacteriol.* **183,** 3383–3390
69. Marchler-Bauer, A., Anderson, J. B., DeWeese-Scott, C., Fedorova, N. D., Geer, L. Y., He, S., Hurwitz, D. I., Jackson, J. D., Jacobs, A. R., Lanczycki, C. J., Liebert, C. A., Liu, C., Madej, T., Marchler, G. H., Mazumder, R., Nikolskaya, A. N., Panchenko, A. R., Rao, B. S., Shoemaker, B. A., Simonyan, V., Song, J. S., Thiessen, P. A., Vasudevan, S., Wang, Y., Yamashita, R. A., Yin, J. J., and Bryant, S. H. (2003) *Nucleic Acids Res.* **31,** 383–387
70. Fellermeier, M. A., Maier, U. H., Sagner, S., Bacher, A., and Zenk, M. H. (1998) *FEBS Lett.* **437,** 278–280
71. Kitajima, J., Ishikawa, T., Fujimatu, E., Kondho, K., and Takayanagi, T. (2003) *Phytochemistry* **62,** 115–120
72. Ershov, Y. V., Gantt, R. R., Cunningham, F. X., Jr., and Gantt, E. (2002) *J. Bacteriol.* **184,** 5045–5051
73. Poliquin, K., Ershov, Y. V., Cunningham, F. X., Jr., Woreta, T. T., Gantt, R. R., and Gantt, E. (2004) *J. Bacteriol.* **186,** 4685–4693